COBEM 2021 26th International Congress of Mechanical Engineering
November 22-26, 2021, Virtual Congress, Brazil

COB-2021-1049
FATIGUE LIFE PREDICTION IN RIGID RISERS WITH CRACK PROPAGATION

Andrielli Nunes Teixeira Pereira
Gilberto Bruno Elwanger
José Renato Mendes de Sousa
PEC/COPPE – UFRJ (Athos da Silveira Ramos Avenue, 149 - Block B, 1st floor - University City of the Federal University of Rio de Janeiro, Rio de Janeiro - RJ, 21941-909, Brazil)
andrielli.nunes@poli.ufrj.br
gbe@laceo.coppe.ufrj.br
jrenato@laceo.coppe.ufrj.br

Silvia Corbani
Escola Politécnica – UFRJ (Athos da Silveira Ramos Avenue, 149 - Block D, 2nd floor - University City of the Federal University of Rio de Janeiro, Rio de Janeiro - RJ, 21941-909, Brazil)
corbani@poli.ufrj.br

Abstract. *Risers are subjected to cyclic and severe environmental loads throughout their service lives. Linear Elastic Fracture Mechanics concepts can be a valuable tool to ensure their safe operation and reduce the conservatism of their designs. This paper presents a methodology for fatigue analysis in rigid risers, including crack nucleation and surface crack propagation. Initially, the global model of the riser is considered with finite beam elements in Orcaflex software loaded to sea states with constant waves. The global fatigue life is determined using stresses, S-N curves, and the Palmgren-Miner rule. The propagation of a pre-existence surface crack at the first weld in the top region of the riser is evaluated by the automatic crack growth technique in FRANC3D software. The remote stresses of three-dimensional models with solid finite element (FE) are obtained from the global model. Stress Intensity Factors (SIF) are computed with the Integral-M method. According to design standards, Newman-Raju closed-form SIF expressions can also be evaluated. Three different cross-section geometries are analyzed with these two approaches. The numerical SIFs for a/t<0.5 are in satisfactory agreement with the Newman-Raju closed-form, but a significant conservatism is found for a/t higher than 0.5. For both approaches, crack front shape and fatigue life are compared.*

Keywords: *Fatigue Life, Fatigue crack propagation, Risers, Finite Element Model.*

1. INTRODUCTION

Marine structures are constantly subjected to cyclic environmental loading. Therefore, fatigue damage shall be evaluated in the design phase to ensure a safe operating margin throughout its service life. There are two modeling methods widely known in literature to predict the fatigue life of welded joints: the crack initiation and the crack propagation methods. The crack initiation corresponds to a large part of the fatigue life, estimated with S-N curves (Hobbacher,2016 and Lotsberg,2016). However, according to Mikulski,2019, the crack propagation method is usually employed to predict the fatigue life of welded joints. In this method, an initial flaw in the welded joint is considered, and fracture mechanics theory and crack growth rate curves are employed to predict the fatigue life. Moreover, the crack initiation phase is disregarded, and only the crack propagation phase is accounted for fatigue life.

Currently, the crack propagation in rigid risers is based on closed-form equations empirically developed to predict the transverse propagation in plates (Newman and Raju, 1981) and the longitudinal propagation in cylinders (Newman and Raju, 1983). The BS7910:2013 standard is based on these closed-form equations, which are widely employed in riser design (Lotsberg,2016). Nevertheless, these equations have limitations, such as the assumption of specific boundary conditions and geometries.

Finite Element (FE) modeling, with the aid of specific crack propagation software, emerges as a tool to overcome the limitations of empirical closed-form solutions. Allied to fracture mechanics, it contributes significantly to the design of more physically realistic analyses by considering the entire stress field acting on the investigated structure, not only the stress peaks (A. Wormsen and G. Härkegård, 2014). Subsequently, the expected results are more accurate and less conservative. Although the computational effort is higher, more robust analyses enable commercial competitiveness and even a possible extension of riser service life with previously detected and analyzed cracks.

The crack growth rate, or crack propagation, depends on the composition of the constituent material and the Stress Intensity Factor (SIF). Therefore, the concepts of Linear Elastic Fracture Mechanics (LEFM) are used to obtain the SIF and the material crack propagation rate curve (da/dN) to evaluate the crack growth.

In this work, the fatigue lives of three different rigid risers are investigated. Firstly, global analyses considering harmonic waves are performed in Orcaflex 10.3 software. Despite the typical use of irregular sea states in these analyses, the sea states are transformed into equivalent regular sea states using the Longuet-Higgins, 1983 procedure to reduce the required computational effort. Next, the fatigue lives of the structures are computed considering the calculated stresses, proper SN curves, and the Palmgren-Miner rule (DNVGL-RP-C203, 2016). After that, two different methodologies are considered to compute the surface crack propagation in these three risers, as outlined in Figure 1.

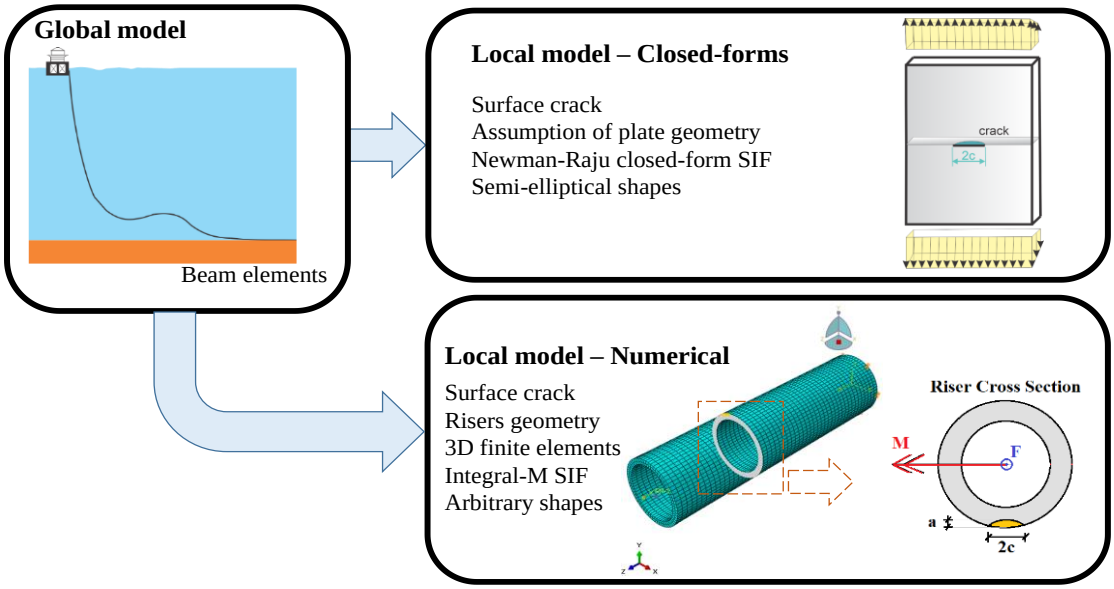

Figure 1. Statement of the problem.

The first local methodology, recommended in the BS7910,2013, assumes a geometric plate shape and a closed-form expression to the SIF, based on Newman and Raju, 1981 (in this work, the crack grows along the riser cross-section plane). The second local methodology relies on three-dimensional FE analyses with the riser cylindrical geometric shape and an arbitrary surface crack. The FRANC3D 6.0.5 (2013) integrated with Abaqus software (2015) are employed to perform these analyses. In this methodology, the numerical method to determine the SIF is the *M*-Integral (Yau et al., 1980). Furthermore, in both methodologies, the initial surface crack is assumed to be a hypothetical flaw with dimensions previously identified on inspection and accepted based on the criteria described in DNVGL-ST-F101.

Therefore, in what follows, the methodologies are described. After that, a case study that encompasses the responses of three different risers is presented to illustrate the application of these methodologies. Finally, the main conclusions of this work are stated.

2. METHODOLOGY

2.1 Fatigue life without crack

The environmental loads considered in global fatigue analyses of rigid risers are due to currents and waves. The wave loading is typically presented in histograms based on environmental studies of the considered region. In fatigue analyses, these histograms consider annual waves, and their percentages of occurrence are also presented. The currents are measured and considered colinear to the current profile.

These loads are employed in global analyses to calculate the forces and moments along the riser. These analyses consider the whole length of the riser, i.e., from the point of connection with the floating unit to its anchoring point. Beam finite elements are employed, and all risers assume the lazy wave configuration (Figure 1). For this configuration, fluctuation modules are used to reduce stresses at the top regions of the structure. This reduction is fundamental in ultra-deepwater fields such as in the Pre-Salt area in Brazil. The global analysis procedure is summarized in Figure 2.

The stresses are obtained in the global analyses, which are used to compute the fatigue damage using SN curves and the Palmgren-Miner rule to accumulate the damage leading to the fatigue life of the structure. In this work, this procedure is only employed to calculate the fatigue damage in the first weld at the top of the riser, which is, usually, the most critical

region. However, it is worth remarking that this procedure disregards initial flaws and, therefore, the concepts of LEFM. This limitation is overcome with the alternative approach presented next.

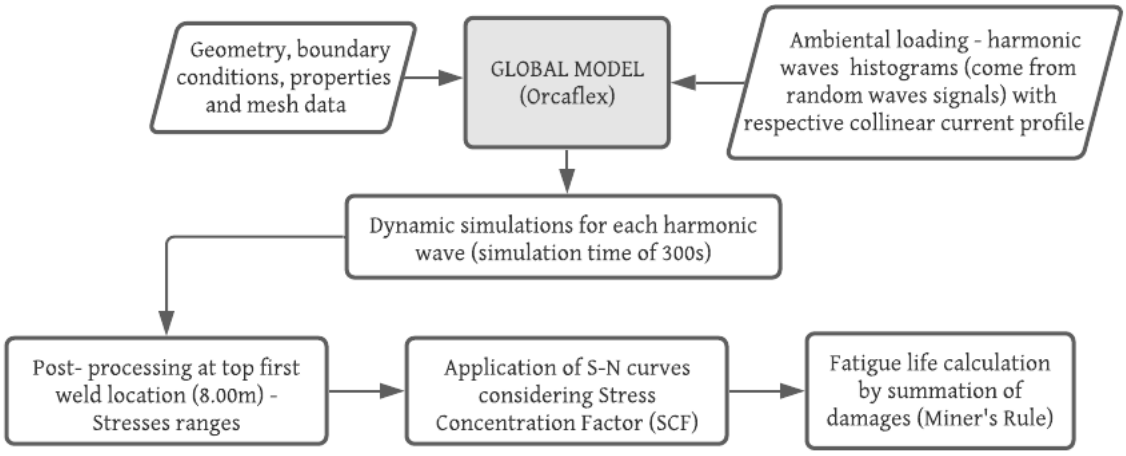

Figure 2. Global analysis procedure of the entire riser (numerical method).

2.2 Fatigue life with crack propagation

The critical region (first weld) is modeled locally with three-dimensional solid finite elements with the aid of the Abaqus software coupled to the pre- and post-processor FRANC3D software. The pre-existing crack is inserted into the FRANC3D software, and its growth is carried out incrementally using the re-meshing technique in the crack region at each step. After automatic incremental growth, it is possible to compute fatigue life according to LEFM theory. In this theory, the SIF range, ΔK, is required to evaluate the crack growth and can be described by Eq. (1)

$$\Delta K = \beta \Delta\sigma \sqrt{\pi a}, \tag{1}$$

where β is the dimensionless geometry factor, $\Delta\sigma$ is the applied remote stress range, a is the depth crack. For riser geometry, numerical analyses are necessary to compute the β factor.

Figure 3 shows the procedure of local analysis (numerical analysis) adopted in this work.

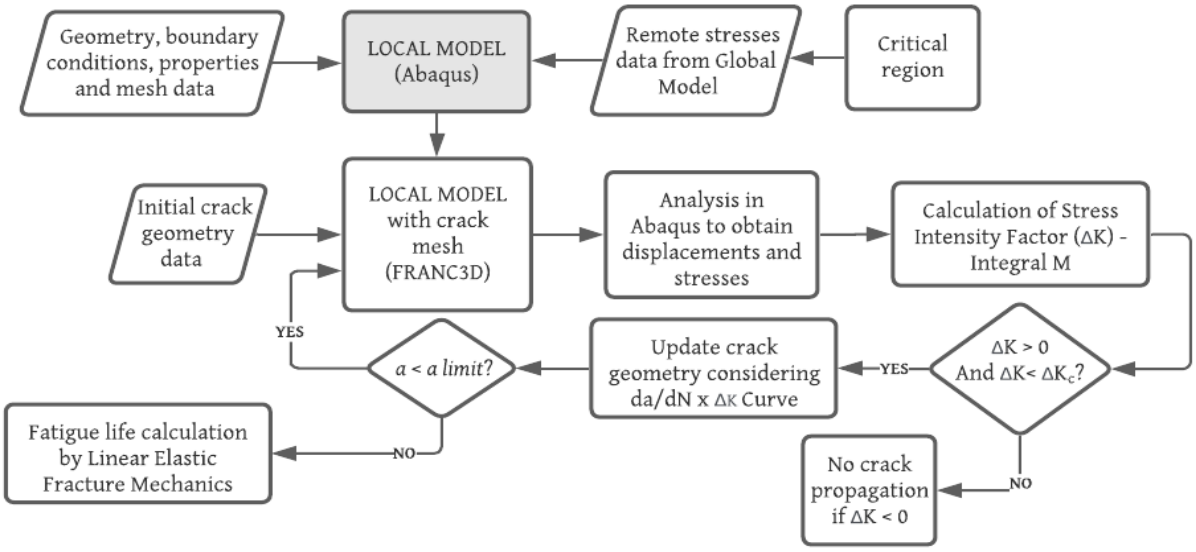

Figure 3. Local analysis procedure of the critical region (numerical method).

The surface crack shape is usually represented by a semi-ellipse when it is on the external surface of the material (Schijve, 2009). However, dividing the crack front into a set of points can be a more accurate approach. In each step of crack growth, ΔN is known, and the maximum crack growth increment, $\Delta_{a,\,max}$, is input at the point of maximum stress intensity factor value, ΔK_{max}, as illustrated in Figure 4. Then, the crack increment at each point i along the crack front, Δa_i, is

$$\Delta a_i = \Delta a_{max} \frac{f(\Delta K_i)}{f(\Delta K_{max})}. \quad (2)$$

where $f(\Delta K)$ is the crack growth rate of the material, and the propagation direction is assumed perpendicular to the crack front. The crack propagation is planar, i.e., perpendicular plane to the applied load, characteristic of Mode I of propagation, with ΔK_I predominant and above the threshold of fatigue crack growth, ΔK_{th}, with Mode II and III of propagation (ΔK_{II} and ΔK_{III}) negligible.

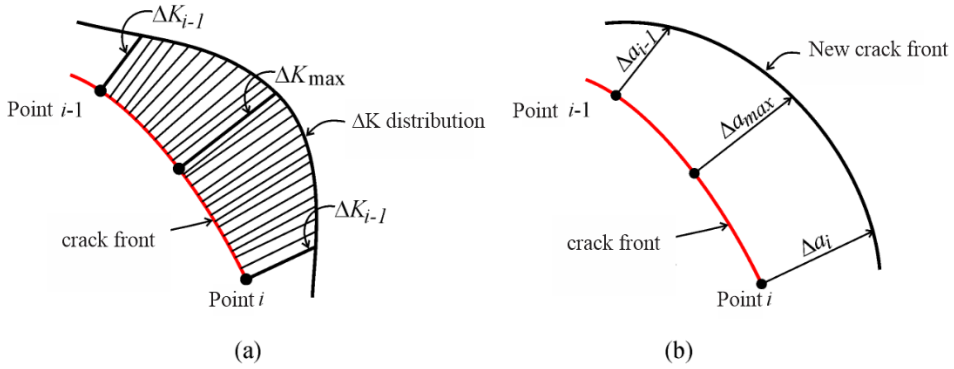

Figure 4. Crack propagation: (a) ΔK along the crack front (b) Δa_i crack increments (Corbani, 2012).

For comparative purposes, crack propagation is calculated with the Newman-Raju closed-form equations (Newman and Raju,1981) and described in current standards used by the industry for rigid riser design (Section 8.4 of BS7910:2013 and DNVGL RP F108). Figure 5 shows the procedure of local analysis using Newman-Raju closed-form.

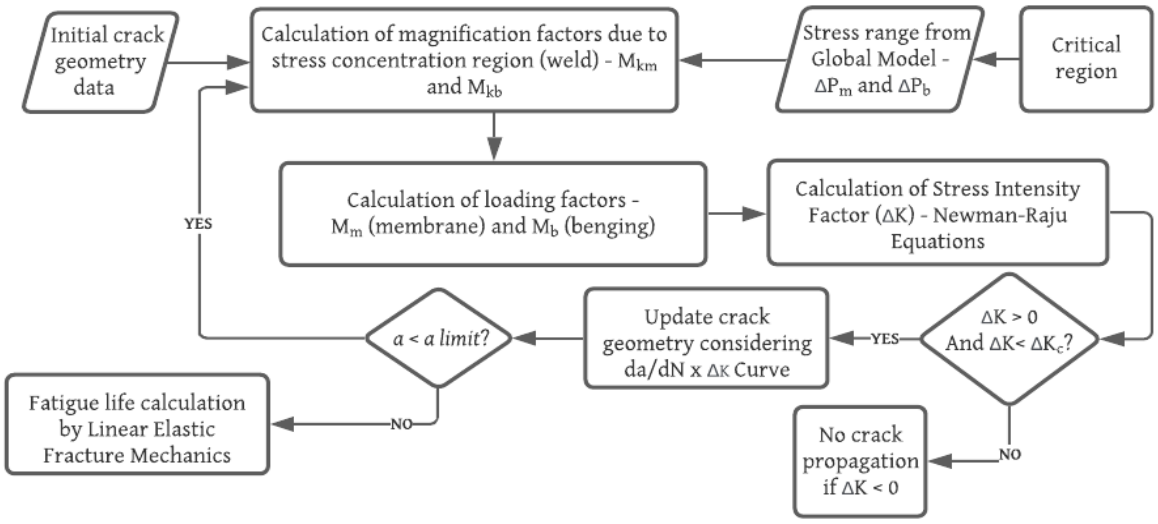

Figure 5. Local analysis procedure of the critical region (Newman-Raju closed-form).

3. CASE STUDY

Three Steel Lazy Wave Risers (SLWR) configurations are studied, as presented in Table 1. They are constituted of X65 carbon steel. The riser sections lengths, the material properties, and the characteristics of the cross-sections are presented in Table 1, Table 2, and Table 3, respectively.

Fatigue life is computed following DNVGL-RP-C203:2016. For the external surface, the shifted B2 curve with cathodic protection was employed, while, for the internal surface, the shifted C curve in the air was used. All parameters of S-N curves are presented in Table 4.

In the global model, the regular waves were applied, as shown in Table 5, where the first row presents wave periods (T in seconds), and the first column presents wave heights (H in meters). The crossing between row and column corresponds to the quantity of the respective pair H x T. This histogram has 451 different load cases in total that include seven main directions. By relying on previous analyses, in this work, only the seven critical waves directions were considered: 0.9 deg, 44.75deg, 83.95deg, 195.1deg, 225.8deg, 271.5deg, and 315.5deg, oriented from True North positive clockwise.

Table 1. Riser Configurations.

	Model 1	**Model 2**	**Model 3**
Hang-off Angle, deg	7	7	7
Water Depth , m	2050	2050	2050
Total Riser Lenght - Nominal, m	3490	3468	3459
TDP Horiz. Distance, m	1420	1377	1342
TRF Horiz. Distance, m	2024	2024	2024
Internal Content Density, kg/m3	820	820	820
HS – Sag Elevation, m	278	241	215
HH – Hog Elevation, m	359	292	248
Sag Horiz.Distance, m	681	696	706
Hog Horiz.Distanc, m	928	902	880
Number of Buoyance Modules (BM), unit	35	40	45
BM Pitch, m	9.5	8.28	7.34
L1 - Bare, m	21	21	21
L2 - Strakes, m	2130	2130	2130
L3 - Bare, m	5	5	5
Lb - Length of Buoyancy Section, m	325	325	325
L4 - Bare, m	15	15	15
L5 - Strakes, m	200	200	200
L6 – Bare, m	794	772	763

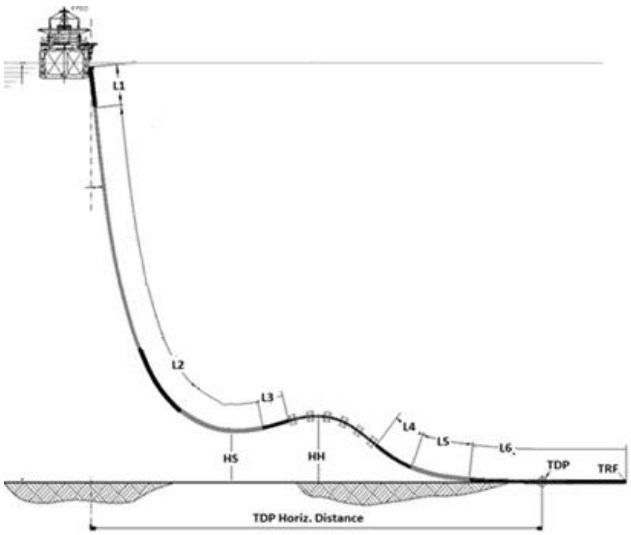

Table 2. Material proprieties.

Properties of Steel X65	
Yield Strength, MPa(1)	427
Ultimate Strength (fu), MPa	531
Young Modulus, GPa	207
K_{th}(threshold SIF), MPa$\sqrt{mm}$(2)	63
K_{max} (maximum SIF), MPa$\sqrt{mm}$(3)	5246

(1) Considering de-rating due the temperature of 100ºC, as per DNVGL-ST-F101. (2) as per BS7910:2013. (3) as per Soares,2011.

Table 3. Riser Cross Sections.

	Model 1	**Model 2**	**Model 3**
Inside diameter, mm	210.6	210.6	210.6
Outside diameter, mm	254.6	266.6	278.6
Wall thickness, mm	22	28	34
Area, mm²	11390	20988	26127

Table 4. S-N curves adopted in global model.

Surface	**S-N curve**	**Low cycle region < N_{lim}**		**N_{lim}**	**High cycle region > N_{lim}**	
		m_1	**log a_1**		**m_2**	**log a_2**
External	B2 shifted with cathodic protection	4	14.685	5.00E+06	5	16.682
Internal	C shifted in air	3	12.592	5.00E+07	5	15.854

The local model is developed initially in Abaqus software with the proper boundary conditions at the upper end and a constant amplitude remote tension and moment loads acting at the lower end. In this model, the geometric properties of the riser cross-sections are considered. In addition, a structured mesh discretization in solid finite elements is considered, and the local riser length is four times the external diameter.

Table 5. Wave histogram considering summation of applied directions.

H(m)/T(s)	2	4	6	8	10	12	14	16	18	20	22	24	26	28	30
1	5494	44242	111856	105661	65221	37459	21079	9801	5077	2708	911	224	41	6	1
2	0	7157	111931	190342	128100	66093	31610	15293	7826	3948	1472	378	74	9	0
3	0	218	36049	61150	49574	29991	13231	5445	2364	1091	473	156	38	2	0
4	0	0	7155	13389	11944	9277	4135	1570	612	260	115	42	9	0	0
5	0	0	910	3162	3001	2715	1337	500	176	65	25	9	1	0	0
6	0	0	91	884	928	868	459	162	49	14	5	0	0	0	0
7	0	0	9	295	343	300	159	50	11	3	0	0	0	0	0
8	0	0	1	110	141	105	52	14	2	0	0	0	0	0	0
9	0	0	0	44	60	36	16	4	0	0	0	0	0	0	0
10	0	0	0	18	27	12	5	0	0	0	0	0	0	0	0
11	0	0	0	7	11	3	1	0	0	0	0	0	0	0	0
12	0	0	0	3	5	1	0	0	0	0	0	0	0	0	0
13	0	0	0	1	2	0	0	0	0	0	0	0	0	0	0
14	0	0	0	0	1	0	0	0	0	0	0	0	0	0	0

Then, the surface crack is inserted in FRANC3D as a semi-elliptical initial shape with semi-axes equal to $2c = 8mm$ (length) and $a = 3mm$ (depth) as illustrated in Figure 6. FRANC3D creates a refined mesh around the crack region for each analysis growth step. The crack front is surrounded by quarter-point elements with different initial aspect ratios for each axis, as indicated in Figure 7. The total degree of freedom, number of elements, and aspect ratios vary with the crack front evolution.

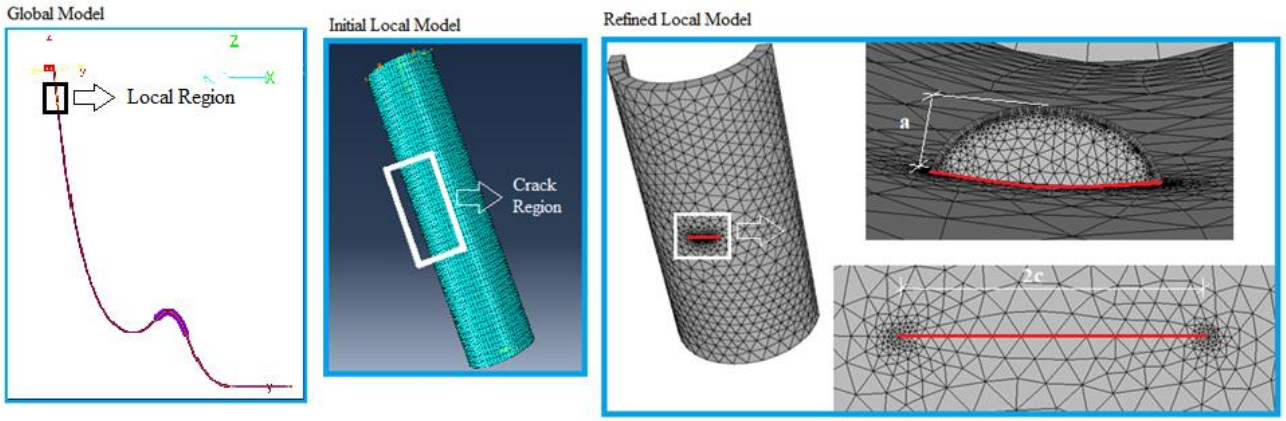

Figure 6. Numerical modeling details.

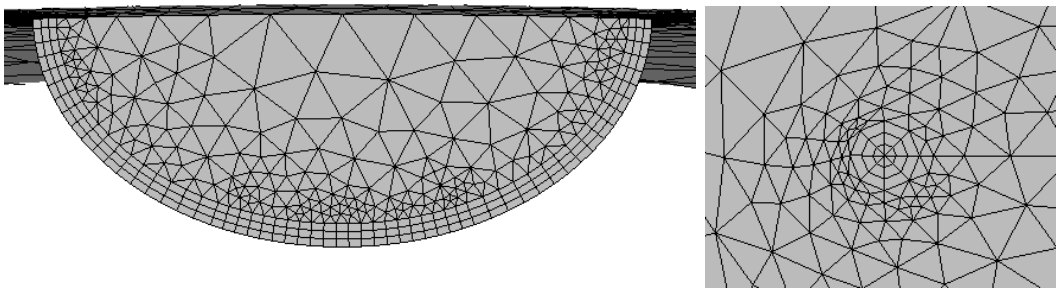

Figure 7. Crack front mesh details.

The crack propagation rate curve, *da*/*dN*, used to compute fatigue life in the local analysis is described in Eq. (3). This curve is a bilinear Paris (1963) according to BS7910:2013.

$$da/dN = A_1 \Delta K^{m_1} \; if \; \Delta K \leq 415MPa\sqrt{mm} \quad \text{and} \quad da/dN = A_2 \Delta K^{m_2} \; if \; \Delta K > 415MPa\sqrt{mm} \tag{3}$$

where, $A_1 = 2.10E^{-17}$, $m_1 = 5.1$, $A_2 = 1.02E^{-07}$ and $m_2 = 1.4$.

4. RESULTS

In global analyses, the damage results are computed at 16 circumferential points: 8 points on the inner surface and 8 points on the outer surface along riser length. Critical total damage and fatigue life are presented in Table 6, which considers the sum of critical damages of each load case with their respective fatigue exposure time. In local analyses, a pre-existent defect is considered in this critical riser region (first weld at the top, which is 8.0 m from the connection).

Table 6. Riser fatigue life in years (S-N curves approach)

	Surface	Overall damage over total exposure time	Total Life (years)
Model 1	External	**1.39E-02**	**72**
	Internal	4.34E-03	231
Model 2	External	8.45E-03	118
	Internal	2.78E-03	360
Model 3	External	5.78E-03	173
	Internal	1.89E-03	529

The remote stress range is extracted from the global analyses to select the critical load case. The axial combined stress came from the resultant stress of maximum tension and bending moment parcels. Thus, the critical load case with the highest axial combined stress is selected to perform the local analyses considering crack propagation. Figure 8 presents the remote stress range at a point 8.5 m from the top connection (immediately below the crack location, 8.0 m). As expected, the thinner riser (Model 1) presents the maximum loads due to its lower resistance to the bending moments.

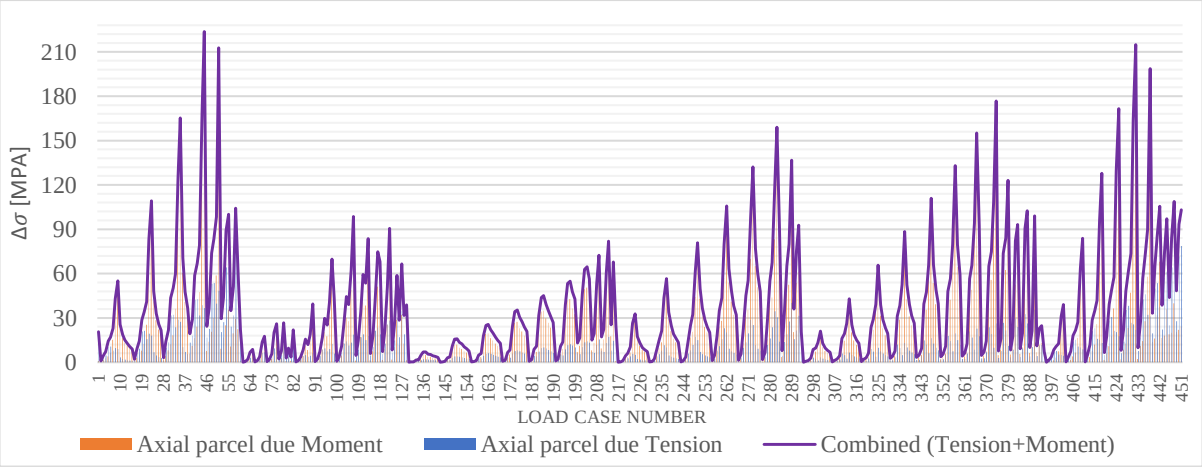

Figure 8. Model 1 - Remote stress range at a point 8.5 m far from the top connection.

Crack growth depends on SIFs and the crack propagation rate curve. This work numerically calculates SIFs with FRANC3D, using the Integral-M method, and by Newman-Raju closed-form solutions, as described in BS7910:2013.

The Newman-Raju closed-form approach is referred to as a plate. Hence, a width and a thickness, respectively, of 280 mm and 28 mm, are considered in Model 2. The oil and gas industry usually applies this British standard in the design of risers. In this work, the Newman-Raju crack shape is evaluated with two approaches:

1) considering magnification factors ($Mk > 1.0$) (weld location, as per annex M.11 of BS7910:2013); and

2) not considering the magnification factor, *i.e.*, $Mk = 1.0$.

The crack length ($2c$) increases faster if the magnification factor M_k is considered (M_k.>1.0), as shown in Figure 9. It is observed that this factor reaches values greater than 2.0 in the crack length; consequently, the value of the SIF at this region is twice higher than the approach that disregards this magnification factor (M_k.= 1.0).

The initial crack geometry starts from a semi-elliptical crack shape for FRANC3D numerical simulation and Newman-Raju calculation (with M_k equal to 1 and higher than 1). The comparison of the crack front shape evolution in Model 2, for example, is shown in Figure 9 for both approaches in every five steps.

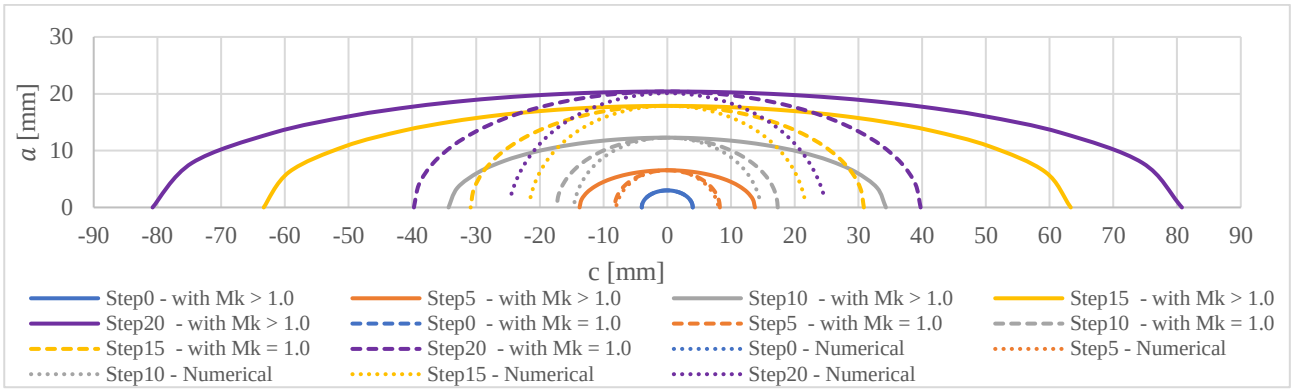

Figure 9. Model 2 - Newman-Raju and numerical crack front shape in every five steps.

From automatic crack growth, the geometry factor (β) along the normalized crack fronts are presented in every five steps in Figure 10. As shown in Table 3, three (3) riser cross-sections with different wall thickness (t) are considered, called: Model 1, Model 2 and Model 3.

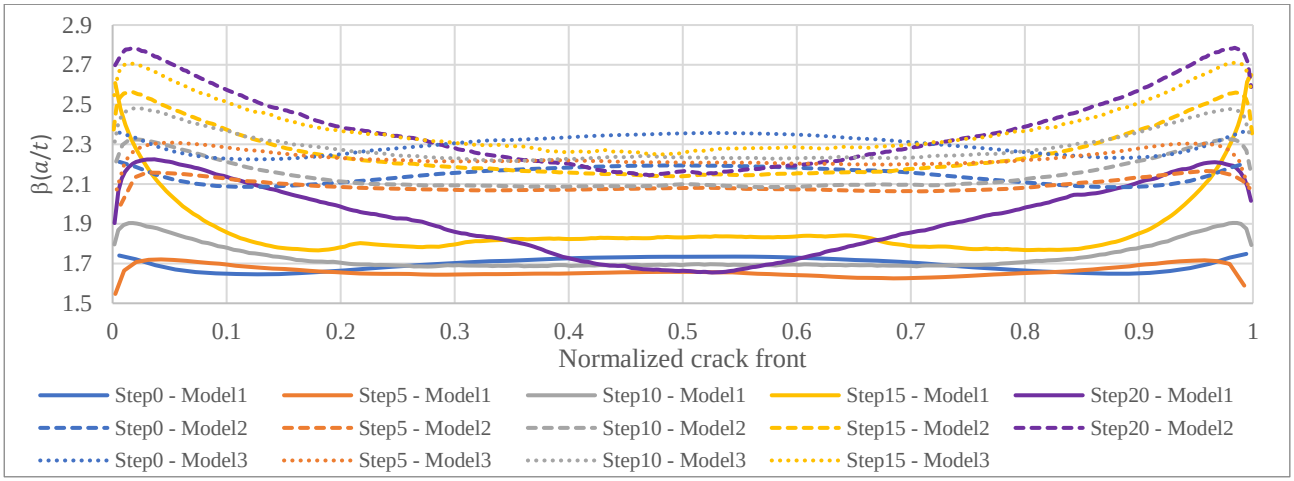

Figure 10. Crack front geometry factor (β) in every five steps – Numerical Models 1, 2, and 3.

The fatigue life is calculated at crack depth evolution, a. For this purpose, a sensitivity analysis of the crack increment (Δa) is performed to demonstrate that Δa led to an accurate number of cycles; for example, Model 1 convergence is shown in Figure 11. Based on FRANC3D results of SIF at this point (crack depth), a polynomial line is adjusted to describe the geometry factor (β), as presented in Figure 12.

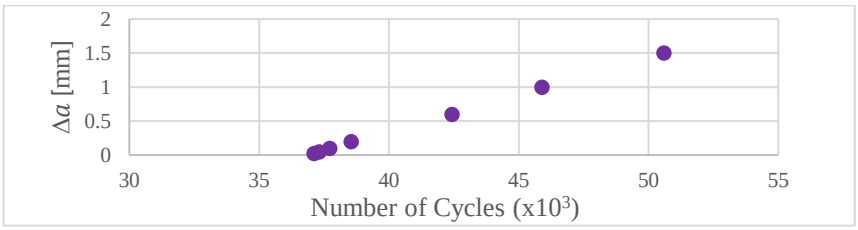

Figure 11. Model 1 - Number of cycles *vs.* crack increments (Δa).

Thus, the fatigue life (N) can be computed by Eq. (1) and Eq.(3) using the critical stress range previously extracted from the global model. An important point observed in Figure 12 is that numerical SIFs for $a/t < 0.5$ are in satisfactory agreement with the Newman-Raju closed-form. However, a significant conservatism is found with a/t higher than 0.5.

Figure 13 compares the fatigue life results, in terms of the number of cycles, for the crack depth of the three analyzed riser configurations using the numerical results and the predictions of Newman-Raju closed-form equations.

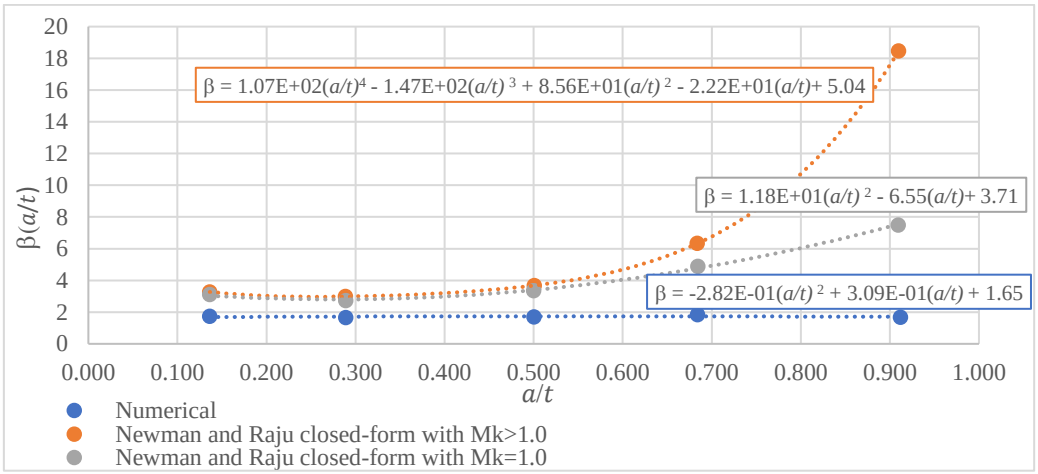

Figure 12. Model 1 - Geometry factor (β) function of crack depth per riser thickness (a/t).

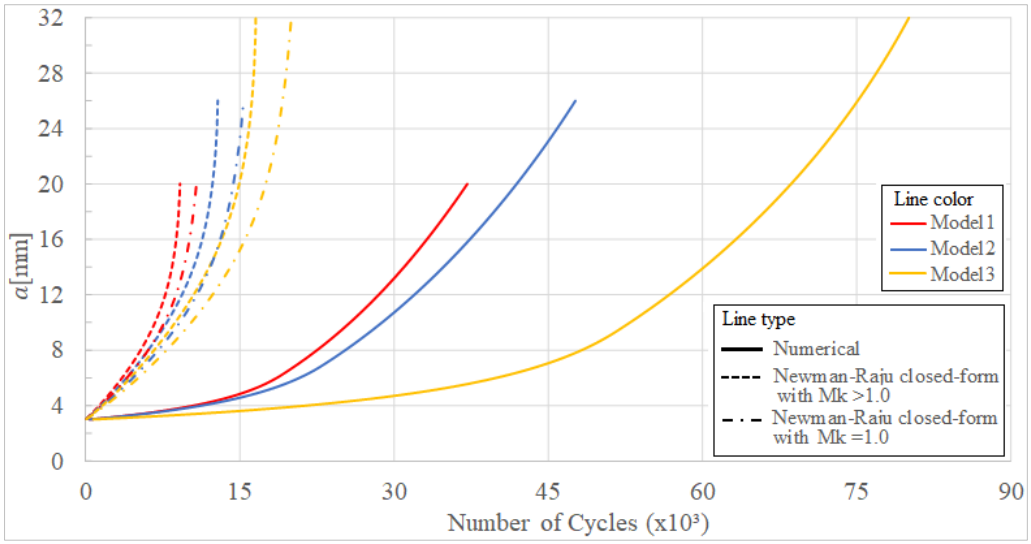

Figure 13. Comparison of fatigue life for the numerical and Newman-Raju closed-form methods.

Table 7 shows the ratio between numerical and other approaches (Newman-Raju closed-form and S-N curve). The complete crack propagation is considered (final depth - Model1: $a = 20mm$; Model2: $a = 26mm$ and Model3: $a = 32mm$) to the critical load case (with highest stress range).

The S-N curve method, added to the Palmgren-Miner rule, present a fatigue life higher than other approaches due crack initiation phase, which corresponds to a large part of fatigue life. However, when an initial flaw is detected in riser, this fatigue life decrease significantly due now only the propagation phase is accounted, as presented in Table 7.

The plastic collapse of the remaining crack section is not evaluated in this paper.

Table 7. Riser fatigue life.

	Number of Cycles (Fatigue Life in years)			**Numerical to other approaches Ratio**		
	Model 1	**Model 2**	**Model 3**	**Model 1**	**Model 2**	**Model 3**
Numerical	37117 (12372 yr)	47629 (15876 yr)	80080 (26693 yr)	1	1	1
Newman-Raju closed-form (with $Mk > 1.0$)	9166 (3055 yr)	12841 (4280 yr)	16540 (5513 yr)	4.05	3.71	4.84
Newman-Raju closed-form (with $Mk = 1.0$)	10763 (3588 yr)	15345 (5115 yr)	19993 (6664 yr)	3.45	3.10	4.01
S-N curve	1195270 (36220)	1992132 (60367)	2883700 (87384)	32.2	41.8	36.0

5. CONCLUSIONS

This paper presented the two methodologies to compute the fatigue life of a rigid riser. Initially, global analyses were performed to identify the critical riser region (first weld at the top). The fatigue life was calculated based on S-N curves and the Palmgren-Miner rule. Thereafter, local analyses were performed using the concepts of LEFM to evaluate the propagation of a pre-existent crack. Crack propagation depends on SIFs, which were calculated by two approaches: closed-form equations and numerical models (Integral-M).

The numerical fatigue life is around four times higher than the fatigue life with closed-form equations (Table 7). This difference shows the conservatism in adopting the Newman Raju closed-form equations, which were developed initially for plate geometry, disregarding the real circular geometry of the riser cross-section. When considering the magnification factor ($Mk > 1.0$) in the closed-form equations calculation, as a weld region was considered, this difference increases (around five times as shown in Table 7). This strategy may allow a more realistic crack growth prediction, which is helpful to calculate the remaining life of these structures in inspection phases.

The fatigue life calculated by the S-N curve to critical load case is much higher than crack propagation approaches – numerical and Newman-Raju closed-forms – (around forty times as shown in Table 7). This difference is due to the crack initiation phase, which demands more time than the crack propagation phase (Schijve, 2009). Thus, a significant impact on the structure fatigue life is perceived when it already presents an initial structural defect (flaw).

6. ACKNOWLEDGEMENTS

The authors would like to thank the members of the Cornell Fracture Group (www.cfg.cornell.edu) for their continued support and for FRANC3D. In addition, the second and third authors are grateful to the Conselho Nacional de Desenvolvimento Científico e Tecnológico (CNPq) for the research grants PQ 311084/2019-2 and PQ 308576/2017-9, which contribute for accomplishing this work. Finally, this study was also financed in part by the Coordenação de Aperfeiçoamento de Pessoal de Nível Superior- Brasil (CAPES), Finance Code 001, and by the Fundação Carlos Chagas de Amparo à Pesquisa do Estado do Rio de Janeiro (FAPERJ).

7. REFERENCES

ABAQUS Version. 6.14: Dassault Systèmes. Simulia Corporation. Providence, Rohde Island, USA.

British Standards Institute, BS7910 Guide to methods for assessing the acceptability of flaws in metallic structures, British Standards Institution, 2013.

CORBANI, S., Propagação de frentes de trincas parcialmente fechadas por flexão cíclica, Tese (Doutorado), Departamento de Engenharia Civil, PUC-Rio, Rio de Janeiro, 2012..

DNV GL's recommended practice, DNVGL-ST-F101 Submarine pipeline systems, Edition October 2017.

DNV GL's recommended practice, DNVGL-RP-C203 Fatigue design of offshore steel structures, Edition April 2016.

FRANC3D 6.0.5. Ithaca (NY, USA): Fracture Analysis Consultants Inc.; 2013. <http://www.fracanalysis.com>.

HOBBACHER A. Recommendations for fatigue design of welded joints and components; 2016.

LONGUET-HIGGINS, M. S. "On the Joint Distribution of Wave Periods and Amplitudes in a Random Wave Field". Proceedings of Royal London Society, A 389, pp 241-258, 1983.

LOTSBERG, I. Fatigue Design of Marine Structures, 1st Edition, Cambridge University Press, New York NY, 2016

MIKULSKI, Z. Fatigue crack initiation and subsequent crack growth in fillet welded steel joints. International Journal of Fatigue 120 (2019) 303–318

NEWMAN, JC and RAJU, IS. An empirical stress intensity factor equation for the surface crack. Engng Fract Mech 1981;**15**:185–92.

NEWMAN, JC and RAJU, IS, "Stress-Intensity Factor for Internal and External Surface Cracks in Cylindrical Vessels Equations" Journal of Pressure Vessel Technology Volume 104 (1983): 293-298

OrcaFlex Manual, 2018, 0b ed. Orcina Ltd. Version 10.3a.

PARIS, PC and Erdogan, F.,A critical analysis of crack propagation laws.Trans.ASME, Series D, Vol. 85 (1963), pp. 528–535.

SCHIJVE, J, Fatigue o Structures and Materials, 2nd Edition, Springer, Holanda, 2009.

SOARES, PA Determination of Fracture Toughness of Api X65 Steel Used in Pipes in the Oil and Gas Industry, M.Sc, Postgraduate Program in Mechanical Engineering at CT-UFES, Vitória, Espírito Santo, 2011

YAU, J.; WANG, S.; CORTEN, H. (1980). A mixed-mode crack analysis of isotropic solids using conservation laws of elasticity. Journal of Applied Mechanics, **47** (June), 335.

WORMSEN, A., HÄRKEGÅRD, G. A novel probabilistic fatigue assessment tool and its application to an offshore riser joint. Procedia Materials Science 3 (2014) 1210 – 1215.

8. RESPONSIBILITY NOTICE

The authors are the only responsible for the printed material included in this paper.